Journal of Medicinal and Nanomaterials Chemistry 2 (2024) 126-142

Journal of Medicinal and Nanomaterials Chemistry

Journal homepage: https://jmnc.samipubco.com/

Original Research Article

Preparation and characterization of CoMo catalyst supported on organized mesoporous zeolite from Kaolin clay

Abimbola George Olaremu*

Department of Chemical Sciences, Adekunle Ajasin University, Akungba-Akoko, Ondo State, Nigeria

ARTICLE INFORMATION

Submitted: 14 December 2023
Revised: 16 February 2024
Accepted: 07 May 2024

Checked for Plagiarism: **YES**
Language Editor checked: **YES**

DOI: 10.48309/JMNC.2024.2.4

KEYWORDS

Kaolin
CoMo/zeolite
Impregnation
Kaolin beneficiation
Clay

ABSTRACT

Zeolites are fascinating materials with a wide range of applications, particularly in environmental and chemical engineering fields. Their porous structure and ion-exchange capabilities make them incredibly useful for tasks like water purification, gas separation, and catalysis. The quest for cheaper raw materials for zeolite synthesis is a significant area of research. Clay minerals, abundant in nature, present a promising alternative to expensive chemical reagents typically used in zeolite production. By harnessing these natural resources, this work is aimed at not only reduce costs but also make zeolite-based technologies that is more accessible and sustainable. This scientific investigation explains the progress of a procedure in producing CoMo supported on zeolite derived from clay. The beneficiated kaolin was transformed into metakaolin at 800 ˚C, followed by leaching with sulphuric acid towards achieving the required silica-alumina ratio for synthesizing zeolite. An alkaline fusion method succeeded in the transformation of metakaolin into zeolite. The impregnation method was selected in incorporating Co and Mo into the zeolite framework. The crystalline phase was identified by EDX, BET, SEM ,and X-ray Diffractometer (XRD) analysis and it showed it contains a zeolite substructure. Fourier Transforms Infrared spectroscopy (FTIR) examination also indicated the existence of zeolite structure and the Energy Dispersive X-ray (EDX) revealed the deposition of Co and Mo onto the surfaces.The presence of Al and Si in the support and Co and Mo as active metals was also confirmed. The results of Transmission Electron Microscopy (TEM), the pore volume and surface area confirmed the synthesis of CoMo/zeolite catalyst, an indication of the possibility of producing CoMo/zeolite from local clay.

Corresponding author, email: abimbola.olaremu@aaua.edu.ng, abimbolaremu@yahoo.com (A.G. Olaremu).

Graphical Abstract

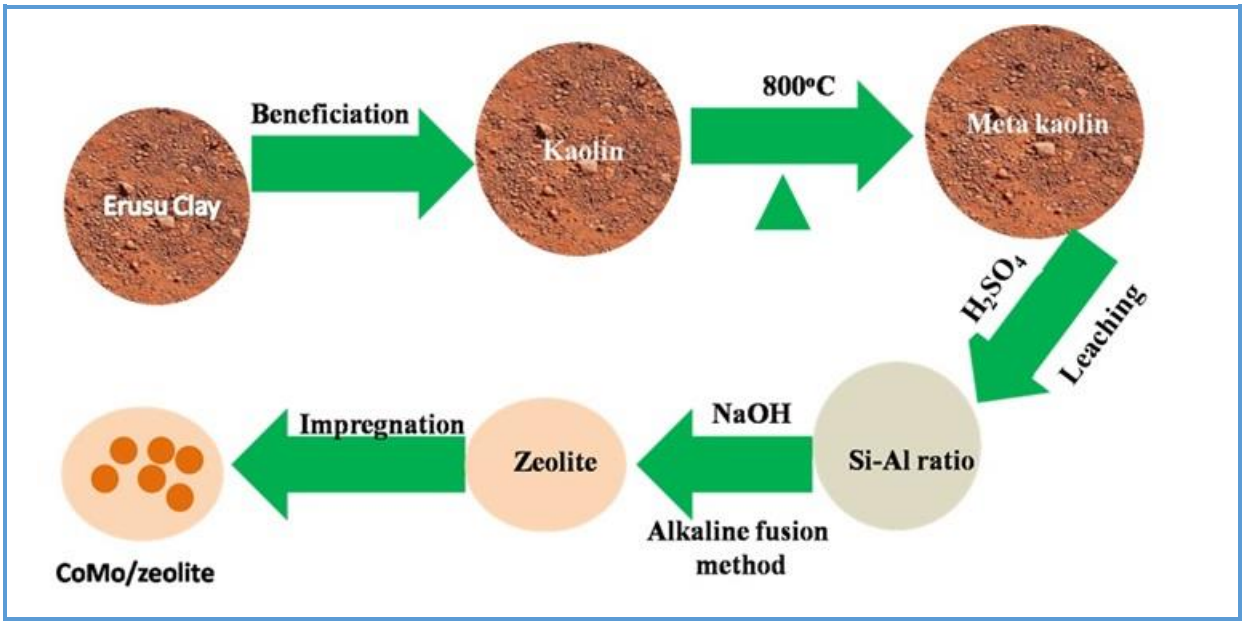

Introduction

Over the years, catalytic cracking processes have evolved in the petroleum sector to refine both light and heavy crude oil. These processes involve breaking down highly complex organic substances like kerogen into lighter hydrocarbon molecules through either thermal or catalytic means[1]. In addition, the need to meet stricter fuel standards and reduce exhaust emissions has led to increased interest in deep hydrodesulphurization (HDS) for removing sulphur moieties from gasoline and diesel oil. To achieve ultra-clean gasoline with very low sulphur content (less than 50 ppm), there is a growing demand for highly potent and selective hydrotreating catalysts that can effectively address refractory polyaromatic sulphur compounds through the hydrodesulphurization (HDS) method [2].

Given that it can give rise to health complications (such as cancer and respiratory problems), air quality in urban areas is a notable problem; the last-mentioned problem is influenced by meteorological pollution to which the gas, (particularly emissions of oxides of sulphur), belched out from vehicles put up in a significant way. To diminish this effect, specifications have been introduced to obtain fuels that are more considerate of the environment [3]. In recent times, the latest environmental regulations concerning fuel standards [4] have made it imperative to enhance the removal of sulphur in diesel through deep hydrodesulphurization (HDS). Since 2009, Europe has set the maximum permitted sulphur concentration in diesel at 10 ppm [3]. The Environmental Protection Agency (EPA) of the United States has also implemented regulations to significantly lower the sulfur and nitrogen content in diesel fuels, lowering them from 500 parts per million weight to 15 parts per million weight and from 300 parts per million weight to 30 parts per million weight in gasoline, initially in 2006 and further to 10 parts per million weight and below in 2009. As a result, several efforts have been made to create more active HDS catalysts,

including looking at various supports and changing the active phase [4]. The hydrodesulphurization (HDS) process for producing ultra-clean fuels from petroleum fractions has garnered significant interest within the heterogeneous catalysis community [5].

Hydrotreatment procedures have a huge interest when the rise in the consumption of fuels is considered, especially, in developing countries and the heterogeneity of the source of the raw materials (mainly from fossil material, lipidic, or lignocellulosic biomass) [3]. Catalytic hydrotreating is one of the most vital procedures in the refineries, utilized to detach nitrogen, compounds of sulphur and oxygen impurities from the feedstock and extensively performed using tungsten sulphide (WS_2) ormolybdenum sulphide (MoS_2) catalyzed by nickel or cobalt deposited on an alumina support. Diverse tactics have been tried to adhere to the many severe environmental standards, such as the use of new supports and active phases or the development of new promoters and additives to be employed for the conventional HDS catalysts. More focus has been placed on one of the unusual materials recently studied as support for HDS catalysts as molecular sieves of the SBA-type mesoporous zeolite [2].

Zeolites are crystalline microporous aluminosilicates characterized by TO4 tetrahedra, where T is typically Al or Si, serving as the primary building blocks. These tetrahedra are interconnected through shared oxygen atoms at their corners, creating intricate three-dimensional framework structures that encompass micropores with diameters smaller than 2 nm [6,7,8]. Zeolites have discontinued being an ingot merely displayed in museums to becomea cost-effective catalyst/catalyst constituents and scientific success-story owing to their extensive uses in industry. This was birthed out as a result of the use of non-natural zeolites in the refinery and petrochemicals [9], and it is seen as a case study of quantum leap and progressive innovation as well as an embodiment of interplay allying science and technology from the foundational academic investigation and the industrial interest to a well-organized macroscale production of zeolites and their distribution in catalytic and adsorbent based procedures. Zeolite possesses great applications which are widely used in petrochemical chemistry, protection of the environment as well as adsorption due to its' high Brunauer-Emmett-Teller (BET) surface area, exuberant acid sites, these materials possess high hydrothermal stability, special framework structure [10]. Zeolites possess unique capabilities and find applications in critical processes such as sorption, separation, water purification, and catalysis, all attributed to their morphology and physicochemical properties. Compared to the conventional y-alumina support, zeolites demonstrate superiority due to their enhanced textural qualities and well-defined pore structure, which includes pore size, shape, and interconnectivity [7]. As excellent catalysts, zeolites are often utilized as substrates for metal nanoparticles to boost their functionality, as they may not individually catalyze every desired reaction effectively.Metal-based nanoparticles are incorporated into zeolitic structures using unconventional techniques such as impregnation, deposition, precipitation, and colloidal synthesis. In addition, state-of-the-art methods are employed to produce composite zeolites with core-shell architectures. These approaches are applied to modulate the acidity, selectivity, and stability of zeolites, enabling bi-functionality during specific catalytic processes [6].

Over the last four decades, zeolite catalysts and metallic composites have played a crucial role in advancing gasoline's octane rating and yield. Furthermore, they have significantly contributed to the development of high-performance lubricants and cleaner fuels, highlighting their widespread impact on various industries [11]. According to [1], catalyst selection for catalytic cracking reactions is influenced by factors such as their regenerative capacity and cost-effectiveness. Zeolite is a prevalent catalyst employed in modern refinery catalytic cracking processes, alongside other catalysts commonly used in the petroleum industry. Zeolites find extensive use in various chemical processes worldwide, including the Fischer-Tropsch process, hydrocracking, catalytic cracking, hydrotreating, and alkylation. Notably, catalysts are manufactured to neutralize harmful substances present in industrial off-gases and vehicle exhaust emissions [12].

The development, application, and performance evaluation of conventional catalysts have spurred extensive and fascinating research investigations. In-depth reviews on the utilization of metallic composites in catalytic cracking reactions hold significant importance, especially for the future advancement of environmentally friendly and economically viable catalysts for oil cracking processes [1]. Khorami and Mansour conducted a study in which they developed a CoMo catalyst supported on multiwall carbon nanotubes (MWCNT). The catalyst's hydrodesulfurization (HDS) activity on naphtha was evaluated using a fixed bed down flow reactor. The results indicated that MWCNT served as excellent support for the HDS catalyst, exhibiting an 88% sulphur conversion based on estimated catalytic activity [5].

The hydrocracking of polyethylene terephthalate was reported by Trisunaryanti *et al.* The characteristics of metal-supported-zeolite catalysts were studied. Characterization results reported demonstrate that the Indonesian natural zeolite consisted majorly of mordenite-type crystalline. The dealumination of the natural zeolite due to the HCl treatment resulted in increased acidity and surface area of the zeolite. Nonetheless, the metal loaded on the zeolite decreased its surface area. The catalyst showed improved performance with 97.99% selectivity towards the gasoline fractions [13]. Sylvette *et al.* utilized amorphous mesostructured ZrO_2 as a support material to disperse the sulphidedCoMo (CoMoS) for hydrodesulfurization (HDS) of 4,6-dimethyldibenzothiophene. It was reported that the dispersed CoMoS over the mesostructured amorphous ZrO_2 support induces a reorganization of the foremost desulphurization procedure, and in that case, a shift towards the direct desulphurization selectivity was obtained [3]. Sepulveda *et al.* investigated the HDS catalytic reaction over rhenium sulphided (ReS_2) catalysts on different supports like zeolite, γ-alumina, and silica. Zeolite-supported ReS_2 catalysts, among these three distinct supports, demonstrated excellent activity when compared with the activities of the other catalysts with the other two supports [14]. Over the years, γ-Al_2O_3 has been the predominant support material for hydrodesulfurization (HDS) and hydrodenitrogenation (HDN) reactions due to its easy availability in the market. However, to enhance acidity and improve catalytic activity, some researchers have explored alternative supports such as silica, carbon, and metal oxides.

Recent studies have shown a growing interest in mesoporous materials as potential catalyst supports. These materials possess

advantages such as increased specific surface area and porosity, making them promising candidates for hydrotreating processes. MCM-41 and SBA-15 are mesoporous materials that have received significant attention in the literature. Reports suggest that catalysts based on Mo, Co, and NiMo supported on MCM-41 exhibit higher activity compared to those supported on y-Al_2O_3. This observation indicates the potential superiority of MCM-41 as a support material for catalytic hydrotreating processes [15]. According to research findings, when compared to conventional catalysts supported on y-Al_2O_3, the performance of Mo, NiW, CoMo, and NiMo catalysts supported on SBA-15 in the sulphided state demonstrated excellent activity for the hydrotreating technique [4]. This indicates that SBA-15, as a support material, holds great promise for enhancing the efficiency of hydrotreating reactions compared to the more commonly used y-Al_2O_3 support. Sami *et al*. (2022) used H-mordenite zeolite for the synthesis of 1,1-diacetates(acylals) of various aromatic aldehydes under solvent-free conditions at room temperature [16].

A recent review focuses on different organic molecules with specific functional groups which can be heterogenized onto silica to synthesize promising catalysts use in industries and biological areas [17]. Previously, Olaremu *et al.* [18] and [11], respectively, synthesized alumina and zeolite from EC. However, there is no systematic study, (to the greatest of our understanding), for the synthesis and characterization of CoMo catalyst loaded on zeolite as support or the study of the catalytic activity of metal catalysts supported on zeolite derived from EC for the catalytic hydrotreating reactions. In this present study, a systematic scheme was developed for the synthesise of zeolite from raw clay and the subsequent loading of metal catalyst and promoter on the manufactured material. Hence, an inexpensive CoMo catalyst supported on zeolite derived from clay was synthesized and reported. This catalyst was characterized using various physicochemical techniques.

Experimental

Sampling and treatment

In this study, the clay sample was collected from Erusu Akoko, located between latitudes 7018'N and 7045'N and longitudes 5031'E to 6006'E. The beneficiation of the clay was conducted using a techniquesimilar to the one described in the reference [18]. Initially, the collected kaolin powder was dried in an oven at 120 °C overnight. This drying process led to the disintegration of the kaolin's framework and the removal of undesired volatile components, resulting in the transformation of kaolin into metakaolin.

Zeolitisation

First, 20 g of metakaolin was added to 250 mL of 2M H_2SO_4 and mixed using a magnetic stirrer for 4 hours at 80 °C for the reaction to take place. Once the reaction was completed, the solution was filtered to recover the residue, which was placed in the oven to dry at 80 °C overnight.The purpose of this process was to remove the structural alumina from the metakaolin using sulphuric acid, aiming to achieve the desired silica-to-alumina mole ratio required for the formation of the desired zeolite. To achieve this ratio, the dried solid obtained previously was combined with 24 g of NaOH in a 1:1.2 ratio. Following the previous step, the mixture was pulverized at 300 rpm for 30 minutes using a ball mill to achieve a uniform solid fusion and calcined at the fusion temperature of 550 °C for 20 minutes. Next, the

calcined material was combined with 150 mL of distilled water and left to preserve (stirred at room temperature) for 24 hours. Afterwards, the mixture was refluxed for 3 hours at 100 °C. Following the reflux process, the mixture was filtered with 10 washes of distilled water before drying in the oven overnight.

Catalyst preparation

The CoMo/zeolite catalyst was prepared using the impregnation method, involving the following steps:

(1) A total of 1.482 g (3 wt. %) of cobalt, obtained from $Co(NO_3)_2.6H_2O$, and 2.576 g (14 wt. %) of molybdenum, obtained from $(NH4)_6Mo_7O_{24}.4H_2O$, were dissolved in 10 mL of de-ionized water. To this solution, 10 g of the synthesized zeolite was added, and the mixture was stirred on a magnetic stirrer for 30 minutes.

(2) The resulting mixture was further stirred and heated at 80 °C and then oven-dried at 120 °C to remove any solvent.

(3) The dried mass of the catalyst, which contained 3 wt. % (1.482 g) cobalt oxide (CoO) and 14 wt. % (2.576 g) molybdenum oxide (MoO_3), obtained through co-impregnation of $(NH4)_6Mo_7O_{24}.4H_2O$ (ammonium heptamolybdate) (Aldrich, 99.98 %) and $Co(NO_3)_2.6H_2O$ (cobalt nitrate hexahydrate) (Aldrich, > 98 %), was subjected to pyrolysis in a muffle furnace at 550 °C for 3 hours.

The resulting catalyst was called CoMo/zeolite and intended for investigation of its catalytic activity in comparison to a commercial zeolite Y catalyst in a separate study.

Characterization

The morphology and elemental content of the Co-Mo/zeolite catalyst were investigated using a Carl Zeiss Evo LS scanning electron microscope (SEM) coupled with energy dispersive analysis of X-ray (EDX) equipment. The infrared spectra of the sample were obtained using the attenuated total reflection (ATR) module of a Nicolet iS5 Thermo Scientific FTIR spectrophotometer. The spectra were captured in the range of 4000 to 500 cm^{-1}. For a closer examination of the catalyst's microstructure, transmission electron microscopy (TEM) images were captured using a JEOL JEM-2010 electron microscope operating at 200 KV. Furthermore, to identify phases and crystallinity of the Co-Mo/zeolite sample, a Thermo Scientific ARL EQUINOX LAUE X-ray Diffractometer was utilized.

In summary, the Co-Mo/zeolite catalyst was thoroughly characterized using various analytical techniques, including SEM-EDAX, FTIR, TEM, and X-ray diffraction, to gain insights into its surface morphology, elemental composition, infrared spectra, microstructure, phase identification, and crystallinity. N_2 gas adsorption and desorption isotherms were used to establish the porosity and specific surface area of the produced catalyst. The measurements of Brunauer-Emmett-Teller (BET) surface area, pore volume, and pore size of the catalyst were taken using the MicroActive for ASAP 2460 version 2.01 analyzer.

Results and Discussion

Kaolin possesses both Si-O and Al-O octahedral and tetrahedral frameworks, but these frameworks are not functional until activation. This implies only one thing which is difficulty in the direct zeolite synthesis. Therefore, the pre-activation of kaolin in order to change this torpid structure must be done.

The most organized technique for activating natural clay involves the thermal transition of

the inert phase into the working phase at elevated temperatures in the presence of alkali hydroxide. Here, this procedure involved the use of a fusion hydrothermal procedure. The clay underwent numerous transitions when it was heated. Metakaolin is a failing phase that retained the tetrahedral silica layers of the initial clay framework. The alkaline fusion process resulted in the formation of zeolites Y, X, and P due to their high reactivity. In this process, kaolin is thermally activated by sodium hydroxide, leading to the production of active Al and Si species. These species act as the basic building blocks for zeolite production, forming discoid frameworks that tend to react with one another to create various zeolite structures [11]. Using Fourier Transform Infrared Spectroscopy (FTIR), the presence of various functional groups in kaolin (clay), zeolite, and CoMo/zeolite was identified, as depicted in Figures 1(a), (b), and (c). The FTIR analysis revealed that kaolin (clay) exhibited characteristic bands at 3697 cm^{-1} and 3620 cm^{-1}, confirming the presence of hydroxyl groups. In addition, it was determined that the octahedral stretch vibrations of kaolinite are associated with OH groups.

In the case of synthetic zeolite shown in Figure 1(b), the FTIR spectra indicated the fundamental vibrations of the tetrahedral framework. Specifically, the peak observed at 1008 c^{m-1} was attributed to the asymmetric stretching of the zeolite's Al-O-Si chain. Moreover, symmetric stretching and bending frequency bands of the Al-O-Si framework were detected at 451 and 695 cm^{-1} and, respectively [19]. In summary, FTIR analysis allowed for the identification of specific functional groups and characteristic vibrations in kaolin, zeolite, and CoMo/zeolite, providing valuable insights into their molecular compositions and structures. The appearance of peaks at 1037, 1020, 1016, and 1417 and 1645 cm^{-1}, in the FTIR spectra were attributed to specific vibrations and linkages. These peaks corresponded to the double-ring external linkage, H_2O vibration, and OH-stretching, respectively [20].

Furthermore, sharp bands observed in kaolin at1008, 1036, and 1110 cm^{-1} were obtained in CoMo/Zeolite. These bands were attributed to Si-O stretching. However, in CoMo/Zeolite, these peaks were observed at slightly different wavenumbers, specifically at 1005 cm^{-1}. Moreover, the presence of a bend (-CH_3) in CoMo/Zeolite was confirmed by the band observed at 1384 cm^{-1}. In summary, the FTIR analysis revealed distinctive peaks associated with specific molecular vibrations and linkages in both kaolin and CoMo/Zeolite, providing valuable information about their functional groups and structures.

EDX analysis, as depicted in Figures 2(a), (b), and (c), was conducted to gain insights into the elemental composition of the catalyst. The EDX study revealed the elements available in kaolin, synthetic zeolite, and CoMo/zeolite. Figure 2(a) presents the elemental compositions of clay (kaolin), as determined by EDX. The investigation demonstrated that the clay is rich in Al and Si, with low levels of Ti and K, and high levels of Fe [22]. These EDX results provide convincing evidence supporting the earlier morphological identification, indicating the prevalence of octahedral particles rich in Na, Al, and Si [23]. The EDX analysis shed light on the elemental composition of kaolin, synthetic zeolite, and CoMo/zeolite, providing valuable information about the presence of various elements and their distribution within the materials. In Figures 2(b) and (c), the EDX spectra of zeolite

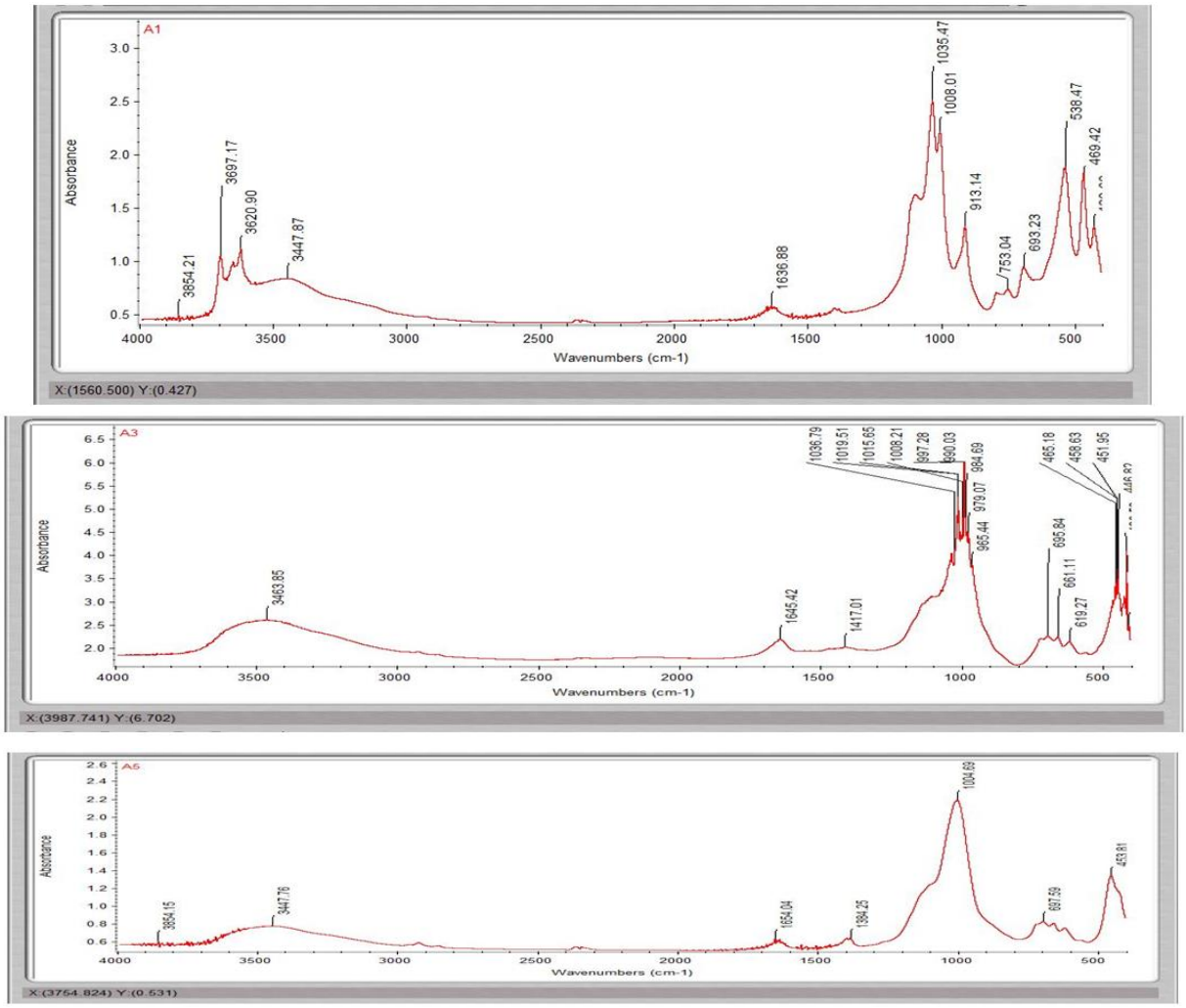

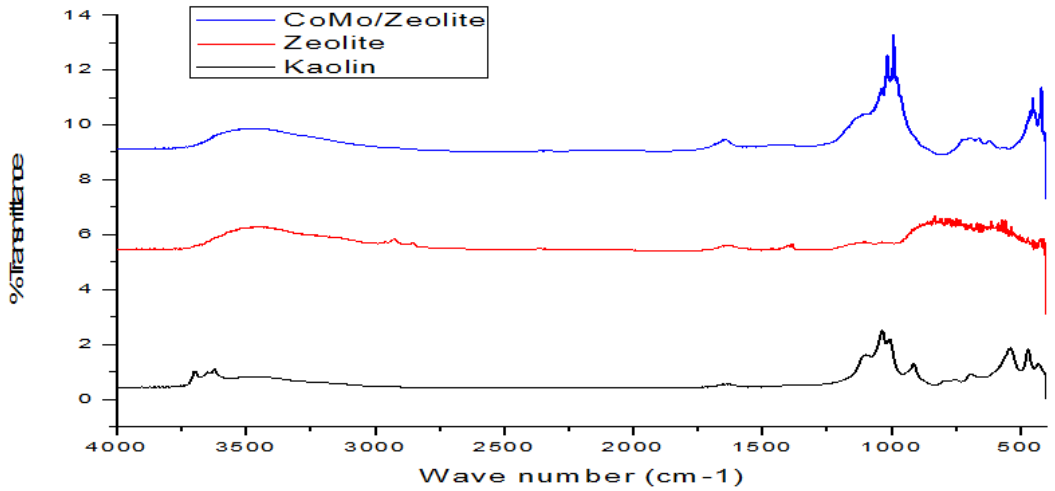

Figure 1. FTIR spectrum of: (a) kaolin, (b) zeolite, (c) CoMo/Zeolite, and (d) summary/combination of a, b, and c.

and CoMo/zeolite were displayed. The EDX analysis of zeolite revealed distinct peaks at energies corresponding to the binding energies of Al, Na, and Si, indicating the presence of these elements in the material. On the other hand, the EDX analysis of CoMo/zeolite exhibited peaks at energies corresponding to Mo, Fe, and Co, providing evidence of the presence of these elements in the CoMo/zeolite sample [21]. Based on the EDX spectra shown in Figures 2(b) and (c), it was established that the primary chemical components of zeolite and CoMo/zeolite were Na, Al, Si, Mo, and trace amounts of K, Fe and Co [24].

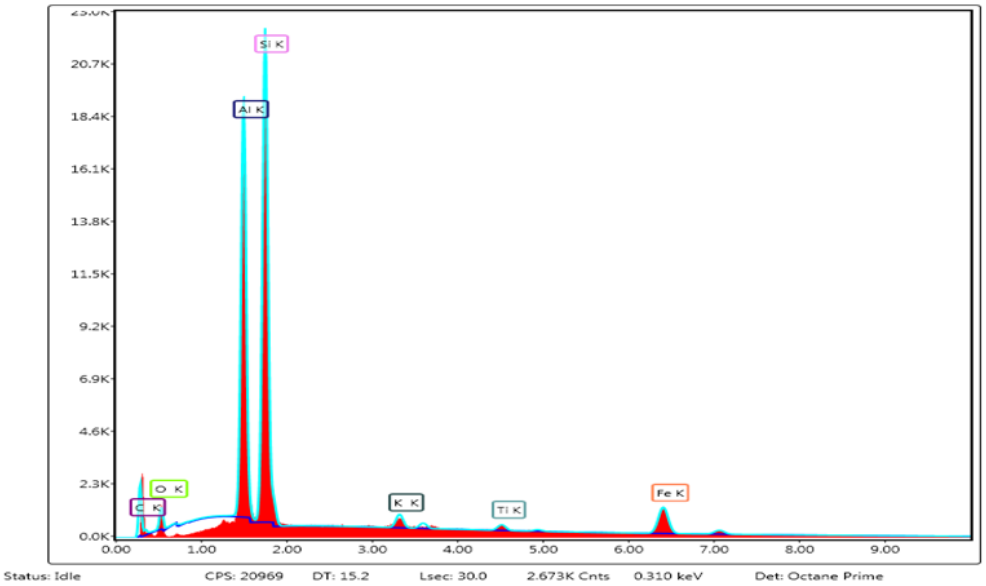

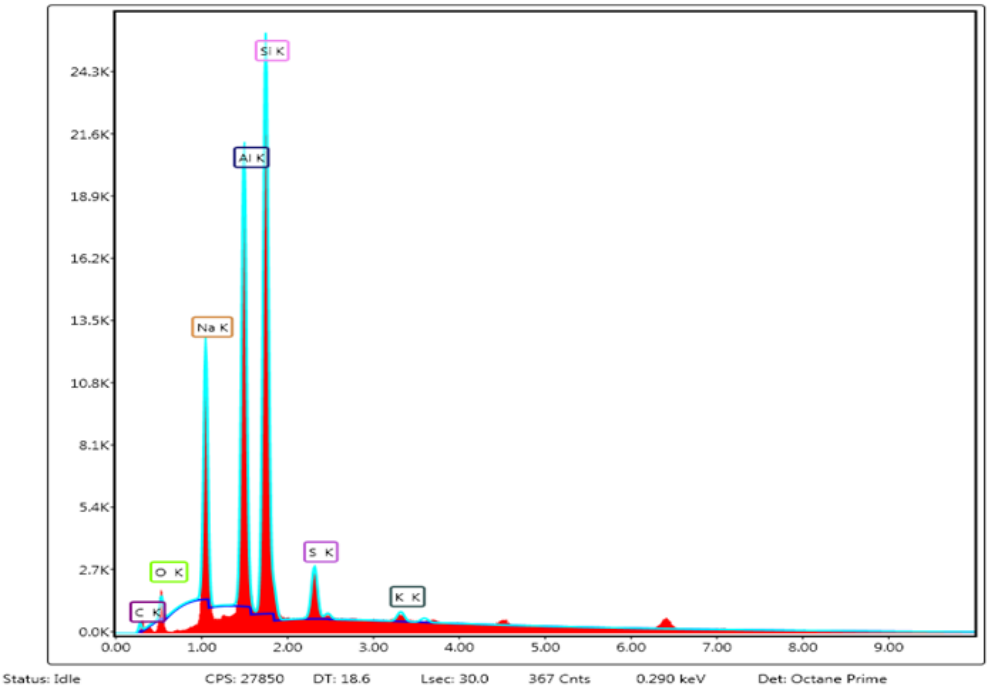

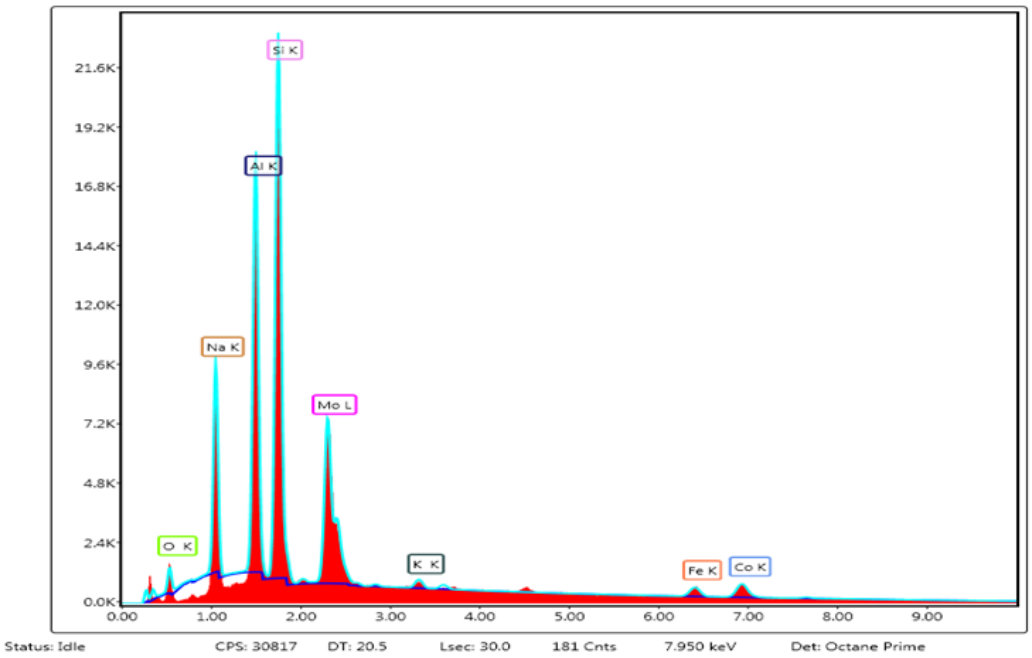

Figure 2. EDX spectrum of (a) clay (kaolin), (b) synthesized zeolite, and (c) synthesized CoMo/zeolite.

This section discusses about the SEM micrographs of kaolin, zeolite, and CoMo/zeolite, as displayed in Figure 3 at a magnification of 100x. In Figure 3(a), the SEM picture of kaolin reveals no discernible change in its surface architecture, showing the morphology of the material. The photograph exhibits a heterogeneous distribution of particles with varying sizes.Comparing the zeolite and CoMo/zeolite samples, certain structural differences can be observed [25]. Zeolite initially possessed narrow pores before modifications were made. In contrast, the structure of CoMo/zeolite appeared to exhibit more looseness after the alterations compared to zeolite [26]. Figure 3(c) illustrates the reduction in pore size after the metal was impregnated with Co and Mo. This reduction is attributed to the ease with which Co and Mo are attached to the catalyst's pores [27]. Based on the SEM measurements, both zeolite and CoMo/zeolite samples displayed relatively similar structures. Both samples showcased a considerable amount of amorphous material along with a small bulk of uniformly dispersed zeolite crystals [28]. These modifications in the CoMo/zeolite sample could be the result of a novel framework produced during the impregnation-based catalyst synthesis of zeolite [25]. In addition, the catalyst's effectiveness is evident, and the CoMo particles were primarily scattered as nanoparticleson the peripheral of zeolite, with some agglomeration observed. The presence of orb-shaped and crushed nanoparticles may essentially enhance the functional surface area of the produced catalyst [25].

In summary, the SEM micrographs provide valuable information about the morphology and structural differences between kaolin, zeolite, and CoMo/zeolite. The impregnation of metal into the catalyst's pores significantly impacted the pore size, while the agglomeration and dispersion of nanoparticles contributed to the catalyst's effectiveness and functional surface area.

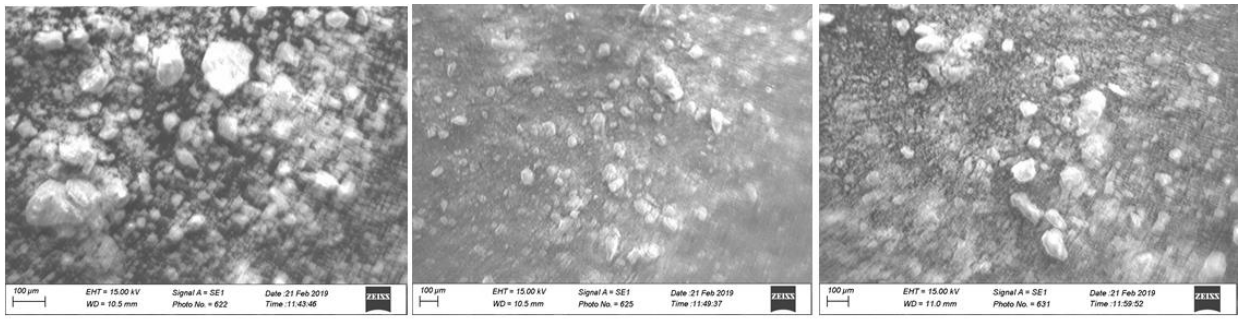

(a) (b) (c)

Figure 3. SEM micrograph of (a) clay, (b) synthesized zeolite, and (c) synthesized CoMo/zeolite.

pyrenes formed through shikimic acid. With the exception of a few rare non-substituted coumarins, all hydroxy and methoxy coumarins have been replaced in the V position [1-4]. The XRD spectral of the synthetic CoMo/zeolite composite was presented in Figure 4, covering a range of 5-40° 2θ. The diffraction peaks observed in this range indicated a highly crystalline zeolite structure [29]. Although the patterns may initially appear less crystalline, they represent the monoclinic $CoMoO_4$ crystalline structure (JCPDS number: 00-021-0868) and the zeolite structure, $Na_5Al_3CSi_3O_{15}/3NaAlSiO_4.Na_2CO_3$ (JCPDS number: 00-015-0469) [30,31]. The CoMo/zeolite catalyst's peaks in Figure 4 were associated with the (111), (331), and (533) planes of the Faujasite Y structure, appearing at Bragg's angles of approximately 6.1°, 15.6°, and 23.5°. The less intense XRD pattern of the catalyst, compared to the supports, suggested that the metals on the zeolite were evenly distributed. This decrease in the crystallinity of the support is commonly observed when active phases are loaded onto it.

The CoMo/zeolite exhibited numerous sharp and distinctive peaks at 2θ values of 24°, 26.4°, and 34.30°, corresponding to the (600), (622), and (664) reflections of the cubic crystalline system and the space group (O). These peaks have been previously documented in the literature [31]. The absence of conclusive evidence linking the phases that should have appeared at 2θ = 23.3° and 27.3° to molybdenum oxide or cobalt oxide made it challenging to identify their level of dispersion. However, the presence of Co and Mo within the zeolite pores caused shifts in the strengths of the Co and Mo peaks. The cobalt peaks were visible at Bragg's angles of 5.0°, 6.1°, and 15.6°, while the sudden appearance of a peak at 35.5° indicated the presence of Mo metal on the catalyst surface [27], the peak 9.7 and 13.6 could be associated with the surface molybdate species. The observed sharp and distinctive peaks at 2θ values between 9 and 20, it indicates that the crystal lattice planes in the material are highly ordered and are giving rise to strong and well-defined diffraction peaks at those particular angles.

In general, the XRD analysis revealed the highly crystalline nature of the CoMo/zeolite catalyst, and its distinctive peaks indicated the presence of specific phases and metals within the zeolite structure. The intensity of the XRD peaks provides valuable information about the degree of crystallinity of the material [32].

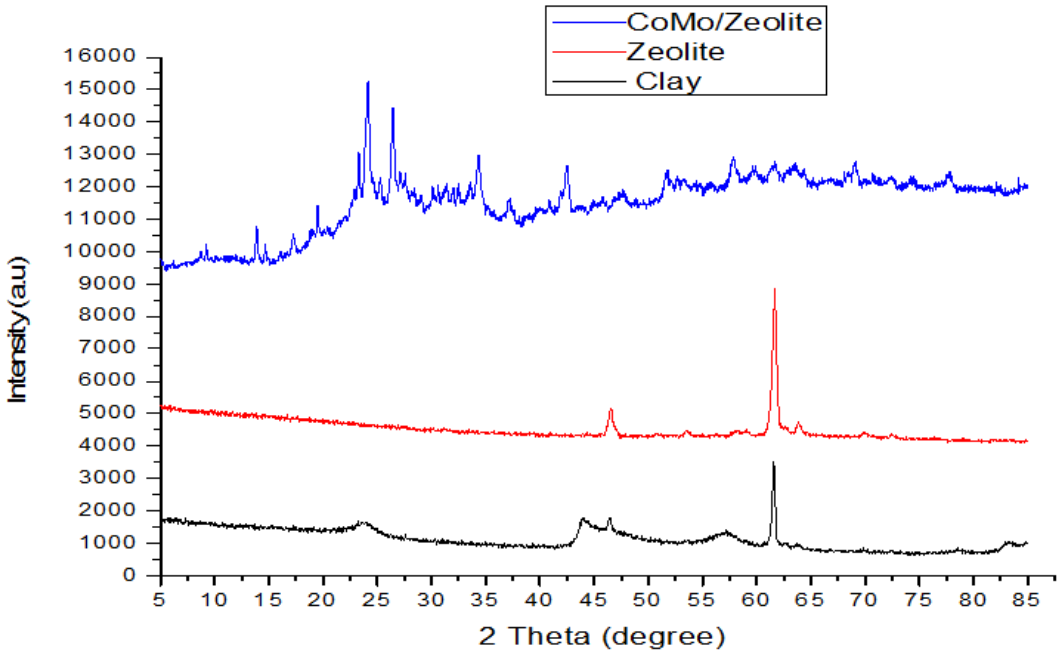

Figure 4. XRD pattern of clay, zeolite, and CoMo/zeolite catalyst.

Figure 5 depicts the N_2 sorption isotherm for CoMo/Zeolite at 77 K, representing the amount adsorbed at STP in cm^3/g of zeolite against p/p^o. The N_2 sorption isotherm was used in conjunction with BET measurements to assess the SSA and pore size of the produced catalyst.In the recent work by Olaremu *et al.* [11], the surface area and average pore size of the as-synthesized zeolite were reported to be 35.7059 m^2/g and 181.3515, respectively. However, in the current study, after modifying the zeolite with Co-Mo, the SSA decreased (26.5995 m^2/g), while the average pore size increased (217.6535). This reduction in surface area was attributed to Co-Mo loadingon the zeolite substrate, indicating that the zeolite's pores were filled with the metals cobalt and molybdenum. Similar observations have been reported in the literature by other researchers [13,27,33].

The N_2 sorption isotherm displayed in Figure 5 corresponds to type IV isotherms in the range of 10^5 p/p^0, which are typical of mesoporous materials [34]. This suggests that the catalyst possesses mesoporous-sized pores [11,36]. The hysteresis loop observed in the isotherm, depicted in Figure 6 [35], is characteristic of type H3 loops, indicative of slit-shaped pores formed by masses of plate-like particles. The presence of flexible aggregates of plate-like particles and the existence of macropores in the pore latticework that are not filled with pore condensate define this type of loop [34]. Therefore, Figure 5 and the accompanying analysis provide valuable information about the N2 sorption isotherm, surface area, and pore size of the CoMo/Zeolite catalyst. The type H3 loop and mesoporous-sized pores observed suggest the presence of specific pore structures within the catalyst. The modification with Co-Mo impacted the surface area and pore size, aligning with findings from other studies in the literature.

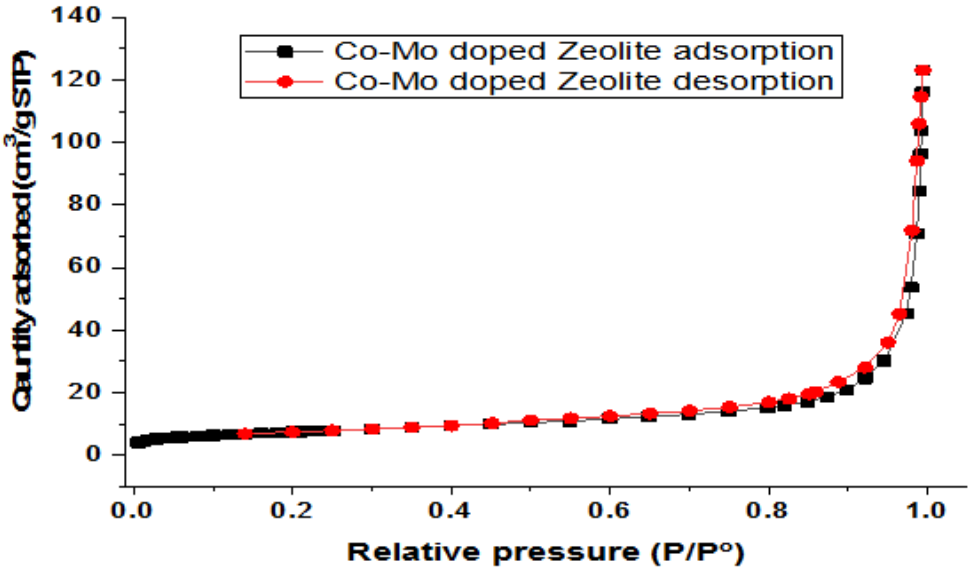

Figure 5. N_2 adsorption-desorption isotherm of Co-Mo doped zeolite.

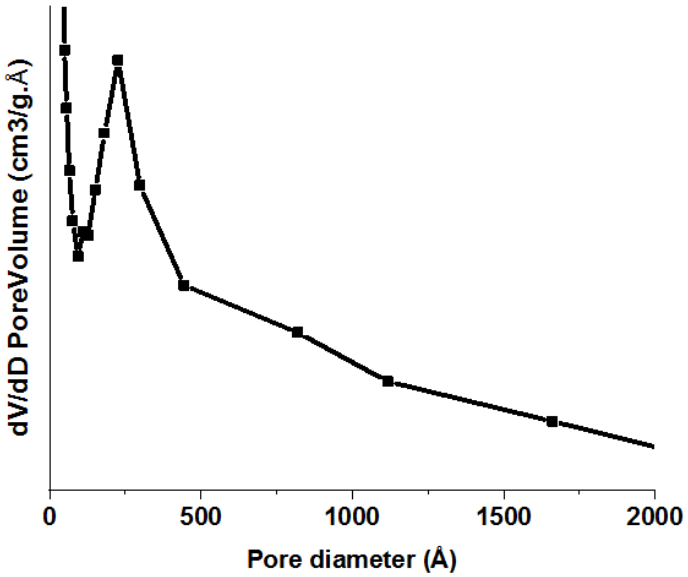

Figure 6. Pore size distribution of CoMo/zeolite.

Figure 7 presents TEM images of the zeolite-supported Co-Mo catalyst evaluated at 500, 100, and 50 nm, respectively [29]. In the sample's micrographs, a clear mesostructure is evident. The TEM images, particularly within the white circles, reveal the presence of a specific multilayered structure in the crystals, displaying some bright lines and bright spots. The bright fields observed in the TEM images are believed to indicate the occurrenceof intraparticle mesopores, which are randomly distributed throughout the crystals [37]. Figure 7 demonstrates the TEM images of the Co-Mo/zeolite catalyst, showing a clear mesostructure and providing valuable insights into the specific layered framework within the crystals, along with the presence of intracrystal mesopores.

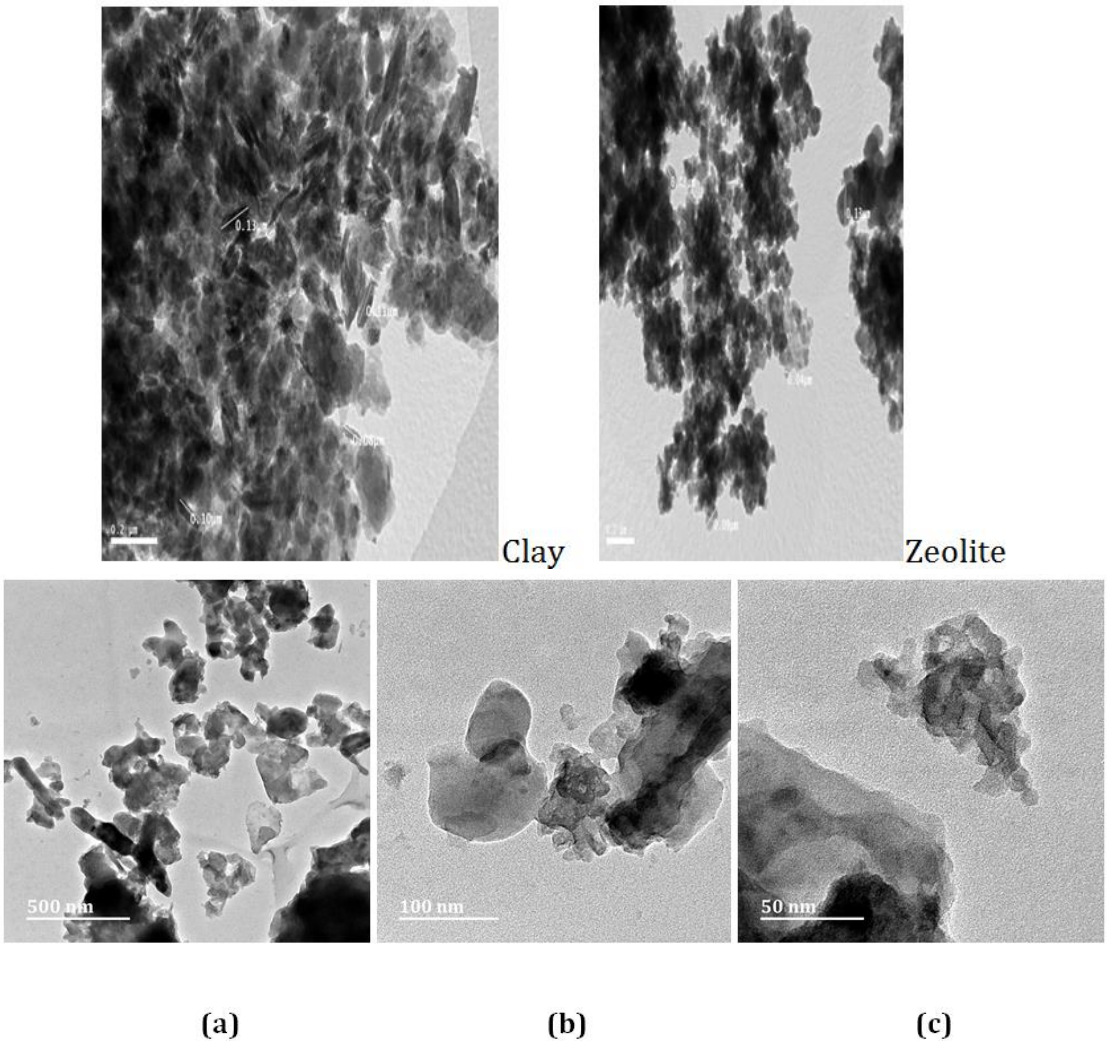

Figure 7. TEM images of clay, zeolite, and synthesized CoMo/zeolite catalyst: (a) 50 nm, (b) 100 nm, and (c) 500 nm magnifications.

Conclusions

The inexpensive functional CoMocatalyst supported on zeolite derived from EC obtained from Erusu-Akoko in Ondo State, Southwestern Nigeria was successfully synthesized after the alkaline treatment of its metakaolin. This study demonstrated the growth of a hydrothermal procedure in developing a vital catalyst (CoMo/zeolite) from the locally available inexpensive clay mineral. It can be concluded that CoMo/zeolite catalyst had been synthesized, an assumption that confirmed the zeolitic substructure by various analytical investigations done on it.

Conflict of Interest

The authors declare that there is no conflict of interest in this study.

Acknowledgements

The authors acknowledged the individuals who contributed to the success of this scientific investigation especially my former student Mr. Adedoyin Rotimi Williams.

Orcid

Abimbola George Olaremu : 0000-0002-8463-7564

References

[1]. Olaremu A.G., Adedoyin W.R., Ore O.T., Adeola A.O. Sustainable development and enhancement of cracking processes using metallic composites. *Applied Petrochemical Research*, 2021, **11**:1 [Crossref], [Google Scholar], [Publisher]

[2]. Gutiérrez O.Y., Pérez F., Fuentes G.A., Bokhimi X., Klimova T. Deep HDS over NiMo/Zr-SBA-15 catalysts with varying MoO_3 loading. *Catalysis Today*, 2008, **130**:292 [Crossref], [Google Scholar], [Publisher]

[3]. Brunet S., Lebeau B., Naboulsi I., Michelin L., Comparot J.D., Marichal C., Rigolet S., Bonne M., Blin J.L. Effect of mesostructured zirconia support on the activity and selectivity of 4, 6-dimethydibenzothiophene hydrodesulfurization. *Catalysts*, 2020, **10**:1162 [Crossref], [Google Scholar], [Publisher]

[4]. Lizama L., Pérez M., Klimova T., Lizama L, Pérez M, Klimova T. A comparison study of NiW and NiPW hydro-desulfurization catalysts supported on SBA-15 and alumina. *Studies in surface science and catalysis (Elsevier)*, 2008, **174**:1251 [Crossref], [Google Scholar], [Publisher]

[5]. Khorami P., Kalbasi M. Hydrodesulphurisation activity of CoMo catalyst supported on multi wall carbon nanotube: sulphur species study. *Journal of Experimental Nanoscience*, 2011, **6**:349 [Crossref], [Google Scholar], [Publisher]

[6]. Juneau M., Liu R., Peng Y., Malge A., Ma Z., Porosoff M.D. Characterization of metal-zeolite composite catalysts: determining the environment of the active phase. *ChemCatChem*, 2020, **12**:1826 [Crossref], [Google Scholar], [Publisher]

[7]. Li K., Valla J., Garcia-Martinez J. Realizing the commercial potential of hierarchical zeolites: new opportunities in catalytic cracking. *ChemCatChem*, 2014, **6**:46 [Crossref], [Google Scholar], [Publisher]

[8]. Adeoye J., Omoleye J. Development of zeolit Y from arobieye mined kaolin. in *3rd International Conference on African Development Issues (CU-ICADI).* 9 [Google Scholar]

[9]. Vermeiren W., Gilson J.P. Impact of zeolites on the petroleum and petrochemical industry. *Topics in catalysis*, 2009, **52**:1131 [Crossref], [Google Scholar], [Publisher]

[10]. Ji Y., Yang H., Yan W. Strategies to enhance the catalytic performance of ZSM-5 zeolite in hydrocarbon cracking: A review. *Catalysts*, 2017, **7**:367 [Crossref], [Google Scholar], [Publisher]

[11]. Olaremu A.G., Odebunmi E.O., Nwosu F.O., Adeola A.O., Abayomi T.G. Synthesis of zeolite from kaolin clay from erusu akoko southwestern. *Journal of Chemical Society of Nigeria*, 2018, **43**: 381[Publisher]

[12]. Naranov E.R., Dement'ev K.I., Gerzeliev, I.M. Kolesnichenko N.V., Roldugina E.A., Maksimov A.L. The role of zeolite catalysis in modern petroleum refining: contribution from domestic technologies. *Petroleum Chemistry*, 2019, **59**:247 [Crossref], [Google Scholar], [Publisher]

[13]. W. Trisunaryanti, Triyono, C.N. Rizki, H. Saptoadi, Z. Alimuddin, M. Syamsiro, K. Yoshikawa. Characteristics of metal supported-zeolite catalysts for hydrocracking of polyethylene terephthalat. *IOSR Journal of Applied Chemistry*, **2013**, *3*, 29-34 [Crossref], [Google Scholar]

[14]. Sepúlveda C., García R., Reyes P., Ghampson I., Fierro J., Laurenti D., Vrinat M., Escalona N. Hydrodeoxygenation of guaiacol over ReS_2/activated carbon catalysts. support and reloading effect. *Applied Catalysis A:*

General, 2014, **475**:427 [Crossref], [Google Scholar], [Publisher]
[15]. Sureshkumar K., Shanthi K., Sasirekha N., Jegan J., Sardhar Basha S. A detailed investigation on rhenium loaded SBA-15 supported catalyst for hydrodenitrogenation reaction of cyclohexylamine. *Journal of Porous Materials*, 2020, **27**:83 [Crossref], [Google Scholar], [Publisher]
[16]. Bhat S.U., Naikoo R.A., Bhat R.A., Malla M.A., Tomar R., Gatum N., Tiwari K. H-mordenite zeolite as an efficient, rapid and recyclable catalyst for chemoselective synthesis of 1, 1-diacetates under solvent-free conditions. *Asian Journal of Green Chemistry*, 2017, **1**:46 [Crossref], [Google Scholar], [Publisher]
[17]. Saoudi M.H., Hello K.M. Antitubercular drugs: new drugs designed by molecular modifications, *Asian Journal of Green Chemistry*, 2022, **6**:370 [Crossref], [Publisher]
[18]. Olaremu A.G. Sequential leaching for the production of alumina from a nigerian clay. *International Journal of Engineering Technology*, *Management and Applied Sciences*, 2015, **3**:103 [Google Scholar]
[19]. Zendehdel M., Khanmohamadi H., Mokhtari M. Host (nano cage NaY)/Mn(II), Co(II), Ni(II) and Cu(II) complexes of *N*,*N*-bis(3,5-di-tert-butylsalicyidene)- 2,2-dimethyle-1,3-diaminopropane, synthesis and catalyst activity. *Journal of the Chinese Chemical Society*, 2010, **57**:205 [Crossref], [Google Scholar], [Publisher]
[20]. Khabuanchalad S., Khemthong P., Prayoonpokarach S., Wittayakun J. Transformation of zeolite NaY synthesized from rice husk silica to NaP during hydrothermal synthesis. *Suranaree Journal of Science and Technology*, 2008, **15**:225 [Google Scholar]
[21]. Salprima Y.S., Adfa M., Falahudin A. Eco-friendly coating of natural zeolite with metallic gold, and characterization of the resulting products. *Oriental Journal of Chemistry*, 2018, **34**:532 [Crossref], [Google Scholar], [Publisher]
[22]. Djeffal L., Abderrahmane S., Benzina M., Siffert S., Fourmentin S. Efficiency of natural clay as heterogeneous fenton and photo-fenton catalyst for phenol and tyrosol degradation. *Desalination and Water Treatment*, 2014, **52**:2225 [Crossref], [Google Scholar], [Publisher]
[23]. Kuwahara Y., Ohmichi T., Kamegawa T., Mori K.,Yamashita H. A novel synthetic route to hydroxyapatite–zeolite composite material from steel slag: investigation of synthesis mechanism and evaluation of physicochemical properties. *Journal of Materials Chemistry*, 2009, **19**:7263 [Crossref], [Google Scholar], [Publisher]
[24]. Cui Y., Zheng Y.,Wang W. Synthesis of 4A zeolite from kaolinite-type pyrite flotation tailings (KPFT). *Minerals*, 2018, **8**:338 [Crossref], [Google Scholar], [Publisher]
[25]. Arimi A., Farhadian M., Solaimany Nazar A.R., Homayoonfal M. Assessment of operating parameters for photocatalytic degradation of a textile dye by Fe_2O_3/TiO_2/clinoptilolite nanocatalyst using Taguchi experimental design. *Research on Chemical Intermediates*, 2016, **42**:4021 [Crossref], [Google Scholar], [Publisher]
[26]. Cheng Q., Li H., Xu Y., Chen S., Liao Y., Deng F., Li J. Study on the adsorption of nitrogen and phosphorus from biogas slurry by NaCl-modified zeolite, *PloS One*, 2017, **12**:e0176109 [Crossref], [Google Scholar], [Publisher]
[27]. Anggoro D.D., Buchori L., Friandani T., Ramadhan Z.R. Effect of Co and Mo metal addition in Co-Mo/Zeolite Y catalyst for coal tar conversion to liquid fuel. *Chemical Engineering Transactions*, 2017, **56**:1717 [Crossref], [Google Scholar]

[28]. Shoumkova A., Stoyanova V. SEM–EDX and XRD characterization of zeolite NaA, synthesized from rice husk and aluminium scrap by different procedures for preparation of the initial hydrogel. *Journal of Porous Materials*, 2013, **20**:249 [Crossref], [Google Scholar], [Publisher]

[29]. Yocupicio R., de León J.D., Zepeda T., Fuentes S. Study of CoMo Catalysts supported on hierarchical mesoporous zeolites for hydrodesulfurization of dibenzothiophene. *Revista Mexicana de Ingeniería Química*, 2017, **16**:503 [Google Scholar], [Publisher]

[30]. Hassanzadeh-Tabrizi S.A., Motlagh M.M., Salahshour S. Synthesis of ZnO/CuO nanocomposite immobilized on γ-Al_2O_3 and application for removal of methyl orange. *Applied Surface Science*, 2016, **384**:237 [Crossref], [Google Scholar], [Publisher]

[31]. Zamani F., Rezapour M., Kianpour S. Immobilization of *L*-lysine on zeolite 4A as an organic-inorganic composite basic catalyst for synthesis of *α*, *β*-unsaturated carbonyl compounds under mild conditions. *Bulletin of the Korean Chemical Society*, 2013, **34**:2367 [Crossref], [Google Scholar]

[32]. Salahudeen N., Ahmed A., Dauda M., Waziri S., Jibril B., Al-Muhtaseb A. Study of the thermal stability effect of impregnation of lanthanum metal on FCC catalyst. *Australian Journal of Industry Research SCIE Journals*, 2014, 10 [Google Scholar]

[33]. Miskolczi N., Juzsakova T., Sója J. Preparation and application of metal loaded ZSM-5 and y-zeolite catalysts for thermo-catalytic pyrolysis of real end of life vehicle plastics waste. *Journal of the Energy Institute*, 2019, **92**:118 [Crossref], [Google Scholar], [Publisher]

[34]. Hernández M.A., Abbaspourrad A., Petranovskii V., Rojas F., Portillo R., Salgado M.A., Hernández G., de los Angeles Velazco M., Ayala E., Quiroz K.F. Estimation of nanoporosity of ZSM-5 zeolites as hierarchical materials. *Zeolites and Their Applications*, 2018, **1**:73 [Crossref], [Google Scholar], [Publisher]

[35]. Ramesh K., Reddy K.S., Rashmi I.,Biswas A. Nanostructured natural zeolite: surface area, meso-pore and volume distribution, and morphology. *Communications in Soil Science and Plant Analysis*, 2014, **45**:2878 [Crossref], [Google Scholar], [Publisher]

[36]. Trunschke A. Surface area and pore size determination. *Modern methods in Heterogeneous catalysis Research*, 2013, 1 [Google Scholar]

[37]. Liu H., Kan Q. Improved performance of hierarchical porous Mo/H-IM-5 catalyst in methane non-oxidative aromatization. *Applied Petrochemical Research*, 2017, **7**:97 [Crossref], [Google Scholar], [Publisher]

How to cite this manuscript: A. G. Olaremu. Preparation and characterization of CoMo catalyst supported on organized mesoporous zeolite from Kaolin clay. *Journal of Medicinal and Nanomaterials Chemistry*, 2024, 6(2), 126-142. DOI: 10.48309/JMNC.2024.2.4